Proceedings of the International Symposium on Planetary Science 2011,
Edited by S. Okano, Y. Kasaba and H. Misawa, pp. 47–58. doi:10.5047/pisps.047

Two-element radio interferometer for the observation of Jupiter's synchrotron radiation

Fuminori Tsuchiya[1], Hiroaki Misawa[1], Hajime Kita[1],
Akira Morioka[1], and Tetsuro Kondo[2]

[1]*Graduate school of Science, Tohoku University,*
Sendai, Miyagi 980-8578, Japan
E-mail: tsuchiya@pparc.gp.tohoku.ac.jp
[2]*National Institute of Information and Communications Technology,*
Kashima, Ibaraki 314-0012, Japan

Observation of the total flux density of Jupiter's synchrotron radiation (JSR) showed a sudden significant flux enhancement on July 14, 1998 associated with an onset of the substorm-like event in the Jovian magnetosphere and it returned to the normal level on the next day. This implies a significant acceleration and transport of high-energy electrons occurred in the inner Jovian magnetosphere. This paper proposes a two-element radio interferometer with a baseline length of a few kilometers to observed changes in spatial distribution of JSR expected to occur during the sudden enhancement event. Two hypotheses are assumed to account for the significant total flux enhancement of JSR: (1) fast radial transport and acceleration of energetic electrons in the equatorial region of the inner magnetosphere and (2) significant enhancement of energetic electrons outside the inner magnetosphere and their injection into the polar region. Spatial distribution of the synchrotron emission is calculated using the electron distribution introduced based on the two hypotheses. While the emission distribution for the hypothesis 1 shows two peaks in dawn and dusk equatorial regions, that for the hypothesis 2 has two peaks in north and south polar regions. It is found that the two-element interferometer with the baseline length of about 3 km along the east-west direction is feasible to detect the difference of emission distributions between two hypotheses.

Key words: Synchrotron radiation, Jupiter's radiation belt, radio interferometer

1 Introduction

Non-thermal particle acceleration in planetary magnetospheres is one of central issues of space plasma and magnetospheric physics. Charged particles accelerated in magnetospheres are trapped in closed magnetic field lines and form radiation belts. In a case of Jupiter, while population of high energy particles extends out radially to 50–100 R_J ($1R_J = 1$ Jovian radius $= 71{,}492$ km), intense radiations are stably trapped in the inner magnetosphere. In this paper, a radiation belt is refereed as an inner magnetospheric region where high energy particles are stably trapped in an internal magnetic field ($L < 10$).

Time variation in high-energy particle flux in Jupiter's radiation belt is difficult to examine by previous in-situ observations because only a few spacecraft and the Galileo probe have observed inside the radiation belt. Jupiter's synchrotron radiation (JSR), which is emitted from relativistic electrons trapped in Jupiter's inner radiation belt, has been used as a probe to observe the time variability of Jupiter's radiation belt. Because the theory of synchrotron radiation is well established, an observation of the synchrotron radiation is a useful tool for remote sensing of relativistic electrons distributed within a few R_J from the planet. Time variations in the total radio flux density of JSR are known for both long-term variation associated with the solar activity and short-term one in the time scale of a few days to a month (Bolton *et al.*, 1989, 2002; Klein *et al.*, 1997; Galopeau *et al.*, 1997; Miyoshi *et al.*, 1999; Misawa and Morioka, 2000; Bhardwaj *et al.*, 2009; Tsuchiya *et al.*, 2010, 2011). Based on previous studies, it is believed that the radial diffusion of trapped electrons dominates both long (de Pater and Goertz, 1994) and short-term (Miyoshi *et al.*, 1999; Santos-Costa *et al.*, 2007, 2008; Tsuchiya *et al.*, 2011) variations in JSR. Though the cause of the short-term variation is still not fully understood, a positive correlation between the short-term change in JSR and the solar UV/EUV flux suggests that it is caused by enhanced radial diffusion driven by the neutral wind in Jupiter's thermosphere (Brice and McDonough, 1973; Miyoshi *et al.*, 1999; Santos-Costa *et al.*, 2007, 2008; Bhardwaj *et al.*, 2009; Tsuchiya *et al.*, 2011).

Recently, Nomura (2008) identified an sudden enhancement in JSR at a frequency of 327 MHz. Upper and middle panels of Fig. 1 show variations in the total flux density of JSR independently observed at the Kiso and Fuji observatories of Nagoya University, respectively, around DOY (day of year) 196 in 1998. A paper which describes details about the observation and data analysis of this event is in preparation. Intensity of JSR suddenly increased by about 10 times as large as that of the usual level on DOY 196 and returned to the previous level within only one day. This time variation can not be explained by the radial diffusion scenario because time scales of the radial transport and the electron loss are order of several tens of days. Fortunately, the Galileo spacecraft orbited around Jupiter in 1998 and measured the magnetic field inside the middle magnetosphere ($\sim 50\ R_J$ from Jupiter) at the time of the sudden enhancement event. The bottom panel of Fig. 1 shows an intensity of magnetic field observed by the Galileo spacecraft. Time variation in the magnetic field with a period of 10 hours is due to the tilt of the magnetic moment axis with respect to the rotation axis by about 10 degrees. Due to the rotation of Jupiter, the spacecraft crosses the magnetic current sheet twice during one planet rotation when it locates around the rotational equator. As the magnetic field magnitude shows maximum when the spacecraft is away from the current sheet, the envelops indicate the intensity of the lobe magnetic field. The figure shows that the lobe magnetic field in the middle magnetosphere gradually increased from DOY 193 to 196 and suddenly decreased at DOY 196. This variation in the lobe magnetic field is interpreted as a signature of the substorm-like event in the Jovian magnetosphere (Ge *et al.*, 2007). The sudden decrease occurred on DOY 196 indicates an onset of the substorm-like event. At the onset of the substorm-like event, injections of energetic electrons and enhancement

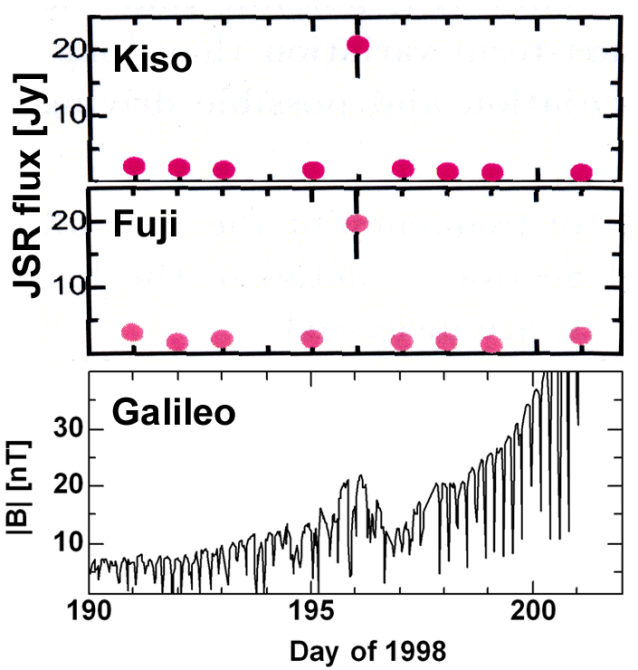

Fig. 1. Upper and middle panels show total flux measurements of JSR independently observed by radio telescopes in the Kiso and Fuji observatories of Nagoya University, respectively. Adopted from Nomura (2008). The bottom panel shows a magnetic field magnitude in the middle Jovian magnetosphere observed by the Galileo spacecraft. The Galileo spacecraft moved from 80 to 15 R_J from the planet during the period shown in the figure. The data is provided from the planetary data system (PDS) in NASA. The envelop of magnetic field data indicates the magnetic field magnitude in the lobe regions.

of low frequency radio waves (hectometric and narrow-band kilometric radiations) were observed by the Galileo spacecraft (Louarn *et al*., 2001). It is interesting to note that the sudden enhancement of JSR was recorded at the onset of the substorm-like event.

Sudden enhancement in the synchrotron radiation shows presence of efficient acceleration and transport of relativistic electrons in the Jovian inner magnetosphere, which occurs associated with the substorm-like event. However, characteristics of the sudden enhancement is not well known because only one event has been observed by single dish radio telescopes so far. In order to investigate basic characteristics of this event, we proposed a two-element radio interferometer with a baseline length of a few kilometers to find changes in the spatial distribution of JSR during the enhancement event. In this paper, we will show a feasibility to detect changes in spatial distribution of JSR during the enhanced event with a two-element radio interferometer.

2 Two-element Interferometer Observations of JSR

To clarify generation mechanisms of the sudden enhancement event of JSR reported by Nomura (2008) (Fig. 1), an interferometer observation is useful to detect changes in spatial distribution of the synchrotron radiation during the event. In this section, we made a feasibility study to observe the sudden enhancement at 325 MHz by using a two-element interferometer, which consists of Iitate Planetary Radio Telescope (IPRT) and a new additional single dish telescope.

2.1 Sensitivity of two-element interferometer

A sensitivity of two-element interferometer is given by the following equation (*e.g.* Wrobel and Walker, 1999):

$$\Delta S_{12} = \frac{1}{\eta_s}\sqrt{\frac{\mathrm{SEFD}_1 \cdot \mathrm{SEFD}_2}{2\Delta f \cdot \tau}}, \tag{1}$$

where SEFD_i is a system equivalent flux density, $i = 1, 2$ are antenna numbers, and η_s is the system efficiency and assumed to be unity. The system equivalent flux density is expressed as follows:

$$\mathrm{SEFD}_i = \frac{2k_B T_{sys,i}}{A_{e,i}}, \tag{2}$$

where $T_{sys,i}$ and $A_{e,i}$ are the system noise temperature and effective aperture area of i-th antenna, respectively. Table 1 shows the sensitivity estimations. IPRT is a single dish radio telescope which measures radio waves in the frequency range from 300 to 800 MHz and was developed at the Iitate observatory of Tohoku University (Iitate village, Fukushima prefecture, Japan; 37°42′N, 140°41′E) (Misawa *et al.*, 2003; Tsuchiya *et al.*, 2010). The antenna of IPRT is composed of two separate rectangular sections whose total physical aperture area is 1023 square meters and installed on an altitude-azimuth mount. Narrow-band receiver systems at 325 and 785 MHz are installed to observed the total flux density of JSR. Recently, a wide-band receiver to measure solar radio emissions in 100–500 MHz range was also installed (Iwai *et al.*, 2012). The aperture efficiency of IPRT is about 65 % for the 325 MHz system and typical system noise temperatures is 150 K. To estimate the sensitivity,

Table 1. Sensitivity of the two-element interferometer which consists of IPRT and a new additional antenna. Specifications of each radio telescope are also shown.

	Spec. of IPRT	Spec. of the new antenna		
Diameter (m)	(32×31.5)	14.6	9.2	6.5
A_e (m^2) ($\eta = 0.6$)	600	100	40	20
T_{sys} (K)	150	150	150	150
SEFD (Jy)	690	4140	10350	20700
ΔS (Jy)		0.12	0.19	0.27

we assume that the new receiving system has the same system noise temperature as IPRT. The band width and integration time are 10 MHz and 10 seconds, respectively. The table shows that the interferometer with a new dish whose diameter is greater than 6.5 m has a sensitivity less than 0.3 Jy (1 Jy $= 10^{-26}$ W cm^{-2} Hz^{-1}). The signal strength output from the interferometer depends on both the baseline length and the distribution of radio sources (see Eq. (3)). As shown in the next section (Fig. 4), the intensity of the cross-correlated signal becomes a half of the total flux density of JSR ($\sim$ 5 Jy) when the baseline length is set to be 3 km. Therefore, the dish diameter of $\geq$ 9 m is feasible to observe JSR with good signal-to-noise ratio of > 10.

2.2 Visibility of JSR during the sudden enhancement event

To calculate the synchrotron radiation distribution, both magnetic and electron distribution models are required. We use a simple centered aligned dipole as a magnetic field model. The synchrotron radiation distribution during the normal state is calculated from an empirical electron distribution model (Garrett *et al*., 2005). In order to explain the significant enhancement of the synchrotron radiation, it is needed to transport and/or generate large number of high-energy electrons in the strong magnetic field region near the planet. We investigate two hypotheses and modify the empirical electron distribution model so as to account for the sudden enhancement of JSR by 10 times as large as the usual intensity.

1. Fast radial transport and acceleration of energetic electrons in the equatorial region of the inner magnetosphere. The electron flux in the empirical model is multiplied by 10 (model 1).

2. Significant enhancement of energetic electrons outside the inner magnetosphere and their injection into the polar region. The electron flux with small pitch angle ($\alpha_{eq} < 10^\circ$ or $\alpha_{eq} > 170^\circ$, where α_{eq} is an equatorial pitch angle) is multiplied by 1000 in the region outside the radiation belt ($L = 6$–15) (model 2).

Both hypotheses assume dramatic changes in the electron distribution near the planet and would not be acceptable under the current understanding on the Jovian magnetosphere. However, we assume that model 2 is more favorable than model 1 because it could explain the fast transport of energetic electrons between the outer part of the magnetosphere and the strong magnetic field region near the planet along the magnetic field line. Because the Garrett *et al*. (2005) model does not support the region outside $L = 16$, $L = 6$–15 is adopted as the region where the electron enhancement occurs in model 2. Figure 2 shows two-dimensional distributions of JSR calculated by using electron flux distributions which are modified based on the assumption introduced in models 1 and 2. The radiation distribution of model 1 (Fig. 2(b)) shows the same shape as that of the Garrett *et al*. (2005) model (Fig. 2(a)), but the intensity is 10 times higher than it. On the other hand, model 2 (Fig. 2(c)) shows a quite different distribution in which the radiations are enhanced in both northern and southern high latitude regions.

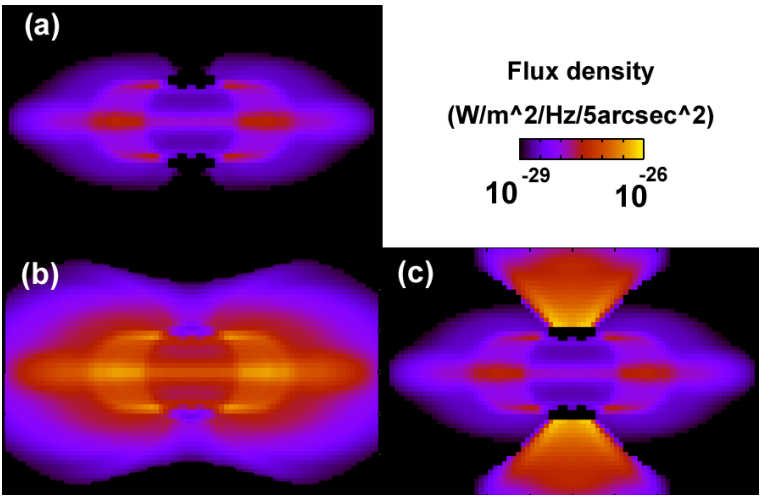

Fig. 2. Two-dimensional distribution of JSR calculated by using electron distributions of (a) Garrett *et al.* (2005) mode, (b) model 1, and (c) model 2. Field of view (FOV) of each panel is 3 arcmin × 2 arcmin. Jupiter is located at the center of each panel.

To examine a feasibility whether the two-element interferometer can distinguish the radiation distributions between models 1 and 2, cross correlation function which is an output from a two-element interferometer is calculated for the emission distributions shown in Fig. 2. It is expected that the degree of the polarization is different between models 1 and 2 because the position angle of the electric field vector seems to be different between the equator and the polar region. Therefore the polarization measurement of JSR by a single-dish telescope could indirectly detect the sudden enhancement at the polar region. In this paper, we focus on the interferometer observation, but will make quantitative estimation of the polarization of JSR in the near future. A cross correlation function, which is also called as a visibility, is calculated as follows (*e.g.* Thompson, 1999):

$$V(u,v) = \int\limits_{\text{source}} \int I(l,m) \exp\left[2\pi i (ul + vm)\right] dl dm, \tag{3}$$
$$u = D_x/\lambda, \quad v = D_y/\lambda,$$

where $I(l,m)$ is the radiation distribution of radio source. $l = \Delta\alpha/\cos\delta$ and $m = \Delta\delta$ are directional cosines along the right ascension α and declination δ, respectively, where $\Delta\alpha$ and $\Delta\delta$ are measured from the center of the radio source. $\mathbf{D} = (D_x, D_y)$ is the baseline vector of the interferometer seen from the radio source and D_x and D_y are the components along l and m, respectively. λ is a radio wavelength. In Eq. (3), it is assumed that each element antenna has the isotropic directivity. The coordinate system used in Eq. (3) is shown in Fig. 3. It is noted that the single dish telescope

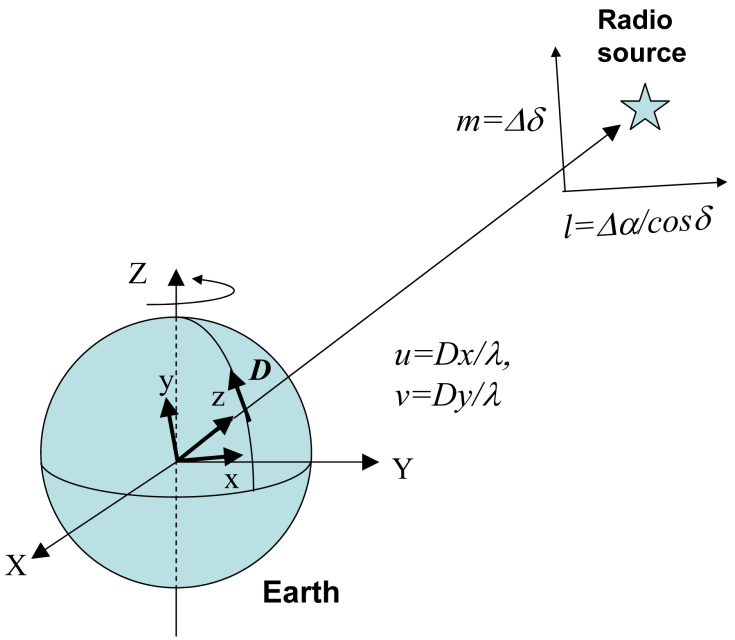

Fig. 3. The coordinate system used to calculate the visibility by Eq. (3). See text in detail.

also measures the visibility at $\mathbf{D} = 0$ ($u = v = 0$) whose amplitude is equivalent to the total flux density.

Figure 4 shows an example of the visibility calculation as a function of the baseline length at the time of Jupiter's southing (*i.e.* hour angle = 0). The baseline is set to be east-west direction. The declination of Jupiter, distance from Earth to Jupiter, and an observation frequency are set to be -15 degrees, 4.04 AU, and 325 MHz ($\lambda = 0.92$ m), respectively. Black and white symbols in the figure indicate the visibility amplitude and phase calculated for models 1 and 2, respectively. The calculation for the normal JSR distribution (gray squares) shows the same visibility phase as model 1 because its radiation distribution has the same shape as model 1. Models 1 and 2 return different interferometer responses. The visibility calculated for model 2 shows a typical pattern of spread single source distribution whose spatial scale is $\lambda/D \sim 1/6{,}000 \sim 30$ arc-sec. This angular size corresponds to a spatial scale of 1–2 R_J. As the two peaks in the emission distribution for model 2 is aligned along north-south direction, two-element interferometer whose baseline is parallel to east-west direction can not distinguish them, that is, they are observed as a single emission source. For model 1 (and the normal JSR distribution), the visibility phase shows 180 degrees around the baseline length of 3 km, which indicates that there are two sepa-

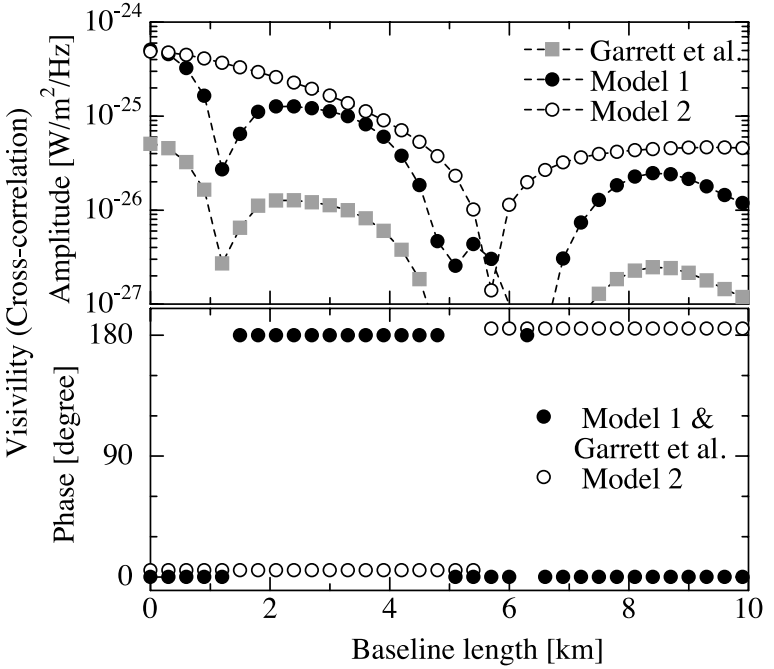

Fig. 4. Visibility amplitude (upper panel) and phase (bottom panel) measured by two-element interferometer as a function of baseline length. The baseline is set to be east-west direction. White and black symbols indicate the result for models 1 and 2, respectively. Gray squares shows the result for the normal JSR distribution (Garrett *et al.* (2005) model)

rate radio sources along east-west direction and the separation is $\lambda/D \sim 1/3{,}000 \sim 1$ arc-min. This corresponds to a spatial distance of $\sim 3R_J$. If the baseline length is chosen in the range from 2 to 4 km, one can easily distinguish differences of the emission distribution between two models by observing the visibility phase.

In a realistic situation, we have to consider some effects which could modify the visibility. First, a baseline vector **D** which is fixed on the ground rotates with respect to the celestial plane as Earth rotates. Second, radio telescopes receive signals which come from radio sources other than Jupiter. This could contaminate the visibility of JSR. In order to consider these two effects, the visibilities of JSR are calculated as a function of the hour angle from -45° to $+45^\circ$. The hour angle range corresponds to the observation time of 6 hours before and after the southing of Jupiter. In order to include radio sources which could contaminate the visibility of JSR, we use the NRAO VLA Sky Survey (NVSS) database. Figure 5 shows distribution of background radio sources introduced in the calculation. As the flux densities of radio sources provided from the database are values at the frequency of 1.4 GHz, they are corrected at the frequency of 325 MHz assuming a spectrum slop of $\alpha = 0.7$ (flux density $\propto f^{-\alpha}$).

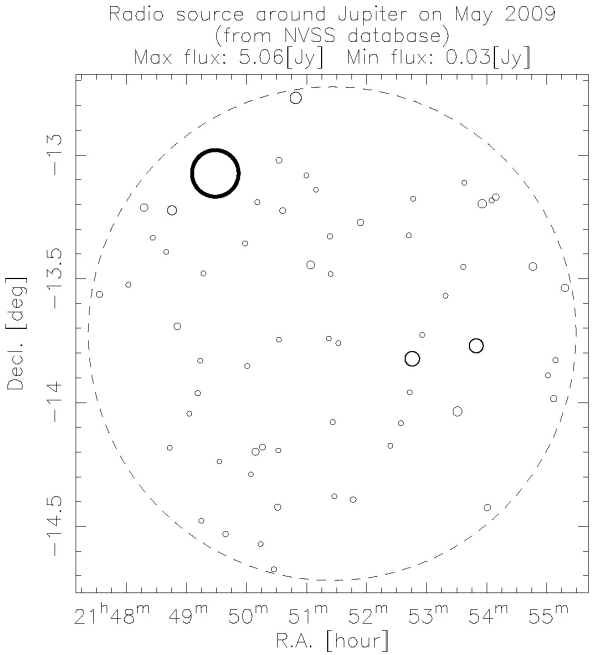

Fig. 5. Distribution of radio sources around Jupiter on May 2009, which is introduced in the visibility calculation of JSR. Size of hollow circles shows represents the flux density of radio sources at 325 MHz. See text in detail.

We also considered a directivity of each element antenna to calculate an antenna temperature of each radio source.

Figure 6 shows changes in the visibility phase as a function of observation time ($\pm$ 3 hours corresponds hour angle range of $\pm$ 45°). We only show a result for a case that the baseline length is 3 km. We again assumed the declination of Jupiter to be $-15°$, distance from the Earth to Jupiter 4.04 AU, and the frequency 325 MHz. Gray squares show the visibility phase for the normal JSR distribution. Although the phase is scattered around 150 degrees due to the contamination from background radio sources, we can identify that it has two separate radio sources along the east-west (dawn-dusk) direction. Black and white circles show the visibility phase as a function of hour angle for models 1 and 2, respectively. The phase values of both models are also scattered around 0 and 180 degrees, but the deviations are small compared with that for the normal JSR distribution because total flux density of models 1 and 2 is 10 times larger than the normal JSR flux density. Crossed symbols also shows a result for model 2, but the electron flux with the small pitch angle is reduced to be one-fifth compared with the original model 2. In this case, total flux density of JSR is three times larger than the normal value. The phase values are scattered around 30 degrees,

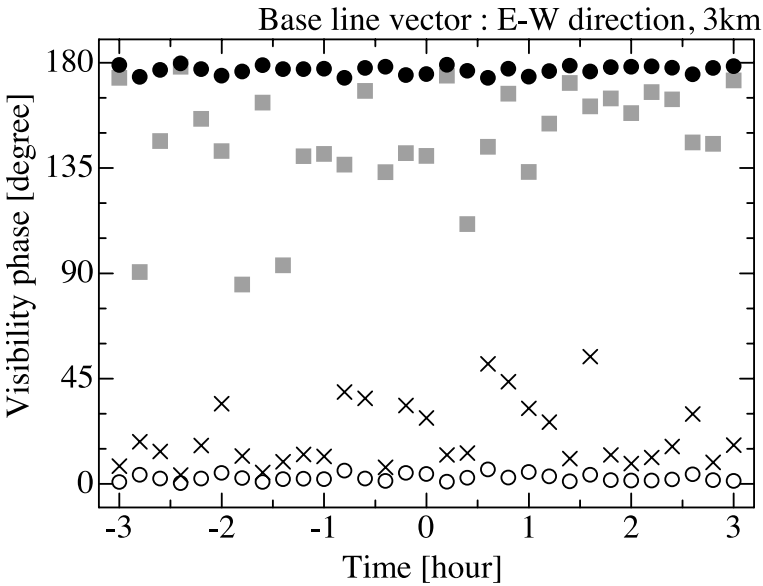

Fig. 6. Variation in visibility phase measured by two-element interferometer as a function of hour angle of Jupiter. The baseline is set to be 3 km along east-west direction. Black and white circles show the visibility phase as a function of hour angle for models 1 and 2, respectively. Gray squares show the visibility phase for the normal JSR distribution. Crossed symbols also shows a result for model 2, but the electron flux with the small pitch angle is reduced to be one fifth compared with the original model 2.

we can still distinguish it from the normal JSR distribution and model 1.

From Fig. 6, it is concluded that the two-element radio interferometer with the baseline of east-west direction and 3 km length can distinguish difference of the emission distributions between the nominal JSR distribution and model 2. We also calculated the visibility of JSR for a case of a single north-south baseline interferometer. However, the visibility phase depends strongly on the hour angle and it is difficult to distinguish model 2 from model 1 (and the normal JSR distribution).

3 Conclusion

We made a feasibility study whether a two-element radio interferometer could identify the change in radio emission distribution expected to occur during the sudden enhancement event of JSR which was reported by Nomura (2008). Two hypotheses are assumed to account for the sudden enhancement of JSR: (1) fast radial transport and acceleration of energetic electrons in the equatorial region of the inner magnetosphere and (2) significant enhancement of energetic electrons outside the inner magnetosphere and their injection into the polar region. Spatial distribution of the synchrotron emission is calculated using the electron distributions introduced by the two hypotheses. In model 2, the synchrotron radiation is expected to have two

separate peaks in north and south polar regions. It is found that the two-element interferometer with the baseline length of about 3 km along the east-west direction is feasible to detect the differences in the emission distribution between two hypotheses. We proposed a two-element radio interferometer with a baseline length of a few kilometers to provide the spatial characteristic of JSR during the sudden enhanced events.

Acknowledgments. This study is supported by the Special Educational Research Budget from the Ministry of Education, Culture, Sports, Science and Technology (MEXT), Japan.

References

Bhardwaj, A., C. H. Ishwara-Chandra, N. Udaya Shankar, H. Misawa, K. Imai, Y. Miyoshi, F. Tsuchiya, T. Kondo, and A. Morioka, GMRT Observations of Jupiter's Synchrotron Radio Emission at 610 MHz, in *The Low-Frequency Radio Universe*, ASP Conference Series, **407**, edited by D. J. Saikia, D. A. Green, Y. Gupta, and T. Venturi, 2009.

Bolton, S. J., S. Gulkis, M. J. Klein, I. de Pater, and T. J. Thompson, Correlation studies between solar wind parameters and the decimetric radio emission from Jupiter, *J. Geophys. Res.*, **94**, 121–128, 1989.

Bolton, S. J., M. Janssen, R. Thorne, S. Levin, M. Klein, S. Gulkis, T. Bastian, R. Sault, C. Elachi, M. Hofstadter, A. Bunker, G. Dulk, E. Gudim, G. Hamilton, W. T. K. Johnson, Y. Leblanc, O. Liepack, R. McLeod, J. Roller, L. Roth, and R. West, Ultra-relativistic electrons in Jupiter's radiation belts, *Nature*, **415**, 987–991, 2002.

Brice, N. M. and T. R. McDonough, Jupiter's radiation belts, *Icarus*, **18**, 206–219, 1973.

de Pater, I. and C. K. Goertz, Radial diffusion models of energetic electrons and Jupiter's synchrotron radiation. 2: Time variability, *J. Geophys. Res.*, **99**, 2271–2287, 1994.

Galopeau, P. H. M., E. Gerard, and A. Lecacheux, Modifications of the synchrotron radiation belts of Jupiter: evidence for natural variations in addition to SL9 effects, *Planet. Space Sci.*, **45**, 1197–1202, 1997.

Garrett, H. B., S. M. Levin, S. J. Bolton, R. W. Evans, and B. Bhattacharya, A revised model of Jupiter's inner electron belts: Updating the Divine radiation model, *Geophys. Res. Lett.*, **32**, L04104, doi:10.1029/2004GL021986, 2005.

Ge, Y. S., L. K. Jian, and C. T. Russell, Growth phase of Jovian substorms, *Geophys. Res. Lett.*, **34**, L23106, doi:10.1029/2007GL031987, 2007.

Iwai, K., F. Tsuchiya, A. Morioka, and H. Misawa, IPRT/AMATERAS—A new metric spectrum observation system for solar radio bursts, *Solar Physics*, **277**, 447–457, 2012.

Klein, M., S. Gulkis, and S. J. Bolton, Jupiter's synchrotron radiation: observed variations before, during and after the impact of comet SL-9, in *Planetary Radio Emission IV*, edited by H. O. Bucker, S. J. Bauer, and A. Lecacheux, 217–224, Austrian Academy Sci., Wien, 1997.

Louarn, P., B. H. Mauk, M. G. Kivelson, W. S. Kurth, A. Roux, C. Zimmer, D. A. Gurnett, and D. J. Williams, A multi-instrument study of a Jovian magnetospheric disturbance, *J. Geophys. Res.*, **106**, 29,883–29,898, 2001.

Misawa, H. and A. Morioka, Observations of Jovian decimetric radiation at a frequency of 327MHz, *Adv. Space Res.*, **26**, 1537–1540, 2000.

Misawa, H., R. Kudo, F. Tsuchiya, A. Morioka, and T. Kondo, Development of a primary feed system for the parabolic rectangular reflector antenna dedicated for planetary radio emission, *Proc. 3rd CRL TDC Symp.*, 57–59, 2003.

Miyoshi, Y., H. Misawa, A. Morioka, T. Kondo, Y. Koyama, and J. Nakajima, Observation of short-term variation of Jupiter's synchrotron radiation, *Geophys. Res. Lett.*, **26**, 9–12, 1999.

Nomura, S., Studies on Variation Characteristics of the Jovian Synchrotron Radiation, Doctor thesis, Tohoku University, 2008.

Santos-Costa, D., S. J. Bolton, R. M. Thorne, Y. Miyoshi, and S. M. Levin, Time Variability of the Jovian Radiation-Belt Emission, in *Abstract of Magnetospheres of Outer Planets Meeting*, San Antonio, 2007.

Santos-Costa, D., S. J. Bolton, R. M. Thorne, Y. Miyoshi, and S. M. Levin, Investigating the origins of the Jovian decimetric emission's variability, *J. Geophys. Res*., **113**, A01204, doi:10.1029/2007JA012396, 2008.

Thompson, A. R., Fundamentals of Radio Interferometry, in *Synthesis Imaging in Radio Astronomy II*, edited by G. B. Talor, C. L. Carilli, and R. A. Perley, BookCrafters Inc., San Francisco, 1999.

Tsuchiya, F., H. Misawa, K. Imai, A. Morioka, and T. Kondo, Multi-frequency total flux measurements of Jupiter's synchrotron radiation in 2007, *Adv. Geosci*., **19**, 601–612, 2010.

Tsuchiya, F., H. Misawa, K. Imai, and A. Morioka, Short-term changes in Jupiter's synchrotron radiation at 325 MHz: Enhanced radial diffusion in Jupiter's radiation belt driven by solar UV/EUV heating, *J. Geophys. Res*., **116**, A09202, doi:10.1029/2010JA016303, 2011.

Wrobel, J. M. and R. C. Walker, Sensitivity, in *Synthesis Imaging in Radio Astronomy II*, edited by G. B. Talor, C. L. Carilli, and R. A. Perley, BookCrafters Inc., San Francisco, 1999.